PHYSICAL REVIEW D **75,** 043002 (2007)

Stochastic background from inspiralling double neutron stars

Tania Regimbau*

Dpt. ARTEMIS, Observatoire de la Côte d'Azur, BP 429 06304 Nice, France

(Received 19 October 2006; published 2 February 2007)

We review the contribution of extra galactic inspiralling double neutron stars, to the LISA astrophysical gravitational wave foreground. Using recent fits of the star formation rate, we show that sources beyond $z_* = 0.005$ contribute to a truly continuous background, which may dominate the LISA instrumental noise in the range $3 \simeq 10^{-4}$–1×10^{-2} Hz and overwhelm the galactic WD-WD confusion noise at frequencies larger than $\nu_o \simeq 2 \times 10^{-3}$.

DOI: 10.1103/PhysRevD.75.043002 PACS numbers: 97.80.−d, 04.30.Db, 95.55.Ym

I. INTRODUCTION

Compact neutron star binaries are among the most promising sources of gravitational waves. At low frequencies, the continuous inspiral signal may be detectable by the space antenna LISA, while ground based interferometers such as VIRGO [1], LIGO [2], GEO [3] or TAMA [4], are expected to detect the last few minutes prior coalescence, at frequencies up to 1.4–1.6 kHz.

In a first paper [5] (hereafter paper I), we have investigated the high frequency signal and its detection with the first generations of ground based detectors. Using new estimates of the mean merging rate in the local universe, that account for the galactic star formation history derived directly from observations and include the contribution of elliptical galaxies, we predict a detection every 148 and 125 years in the volume probed by initial VIRGO and LIGO, and up to 6 detections per year in their advanced configuration.

In a second paper [6] (hereafter paper II), we used numerical simulations to estimate the gravitational wave emission produced by the superposition of unresolved extragalactic sources. As in paper I, we were interested in the few 16 minutes before the last stable orbit is reached, when more than 96% of the gravitational wave energy is released and when the frequency evolves in the range 10–1500 Hz, covered by ground based interferometers. We find that above the critical redshift $z_* = 0.23$, the sources produce a truly continuous background, with a maximal gravitational density parameter of $\Omega_{\rm gw} \simeq 1.1 \times 10^{-9}$ around 670 Hz. The signal is below the sensitivity of the first generation of ground based detectors but could be detectable by the next generation. Correlating two coincident advanced-LIGO detectors or two third generation EGO interferometers, we derived a S/N ratio of 0.5 and 10, respectively.

In this article, we extend our previous simulations to investigate the stochastic background from the early low frequency inspiral phase. Estimates of the emission from the various population of compact binaries (see for instance [7–12] for the galactic contribution and [13–15] for the extragalactic contribution) or from captures by supermassive black holes ([16]), which represent the main source of confusion noise for LISA, are of crucial interest for the development of data analysis strategies. The paper will be organized as follow. In Sec. II, we describe the simulations of the double neutron star (DNS) population, in Sec. III. the contribution of inspiralling DNS to the stochastic background is calculated and compared to the LISA instrumental noise and to the white dwarf-white dwarf (WD-WD) galactic foreground. Finally, in Sec. IV the main conclusions are summarized.

II. SIMULATIONS OF THE DNS POPULATION

To generate a population of DNSs (each one characterized by its redshift of formation and coalescence timescale) we follow the same procedure as in paper II, to which the reader is referred for a more detailed description.

The redshift of formation is randomly selected from the probability distribution [17]:

$$P_f(z_f) = \frac{R_{zf}(z_f)}{R_p} \tag{1}$$

constructed by normalizing the differential DNS formation rate,

$$R_{zf}(z_f) = \frac{dR_f(z_f)}{dz_f}. \tag{2}$$

The normalization factor in the denominator corresponds to the rate at which massive binaries are formed in the considered redshift interval, e.g.,

$$R_p = \int_0^6 (dR_f(z_f)/dz_f) dz_f, \tag{3}$$

which numerically gives $R_p = 0.044\ \mathrm{s}^{-1}$ in the two cosmic star formation rate adopted in this paper.

The formation rate of massive binaries per redshift interval Eq. (2) writes:

$$R_{zf}(z_f) = \lambda_p \frac{R_f^*(z_f)}{1+z_f} \frac{dV(z_f)}{dz_f}, \tag{4}$$

*Electronic address: regimbau@obs-nice.fr

where $R_f^*(z)$ is the cosmic star formation rate (SFR) expressed in $M_\odot$ Mpc^{-3} yr^{-1} and λ_p is the mass fraction converted into DNS progenitors. Hereafter, rates per comoving volume will always be indicated by the superscript "*", while rates with indexes "z_f" or "z_c" refer to differential rates per redshift interval, including all cosmological factors. The (1 + z) term in the denominator of Eq. (4) corrects the star formation rate by time dilatation due to the cosmic expansion.

The element of comoving volume is given by

$$dV = 4\pi r^2 \frac{c}{H_o} \frac{dz}{E(\Omega_i, z)} \tag{5}$$

with

$$E(\Omega_i, z) = [\Omega_m(1+z)^3 + \Omega_v]^{1/2}, \tag{6}$$

where Ω_m and Ω_v are, respectively, the present values of the density parameters due to matter (baryonic and nonbaryonic) and vacuum, corresponding to a nonzero cosmological constant. Throughout this paper, the 737 flat cosmology [18], with $\Omega_m = 0.30$, $\Omega_v = 0.70$ and Hubble parameter $H_0 = 70$ km s^{-1} Mpc^{-1} [19] is assumed.

Recent measurements of galaxy luminosity function in the UV (SDSS, GALEX, COMBO17) and far-infrared (FIR) wavelengths (Spitzer Space Telescope), after dust corrections and normalization, allowed to refine the previous models of star formation history, up to redshift $z \simeq 6$, with tight constraints at redshifts $z < 1$. In our computations, we consider the recent parametric fits of the form of [20], provided by [21], constrained by the Super Kamiokande limit on the electron antineutrino flux from past core-collapse supernovas. It is worth mentioning that the final results are not significantly different if we adopt, as in paper II, the SFR given in [22].

Throughout this paper, we assume that the parameter λ_p does not change significantly with the redshift and can be considered as a constant. In fact, this term is the product of three other parameters, namely,

$$\lambda_p = \beta_{\rm NS} f_b \lambda_{\rm NS}, \tag{7}$$

where $\beta_{\rm NS}$ is the fraction of binaries which remains bounded after the second supernova event, f_b is the fraction of massive binaries formed among all stars and $\lambda_{\rm NS}$ is the mass fraction of neutron star progenitors. From paper I we take $\beta_{\rm NS} = 0.024$ and $f_b = 0.136$. [21] investigated the effect of the initial mass function (IMF) assumption on the normalization of the SFR. They showed that top heavy IMFs are preferred to the traditional Salpeter IMF [23] and their fits are optimized for IMFs of the form:

$$\xi(m) \propto \begin{cases} \left(\frac{m}{m_0}\right)^{-1.5} & \text{for } 0.1 < m < m_0 \\ \left(\frac{m}{m_0}\right)^{-\gamma} & \text{for } m_0 < m < 100 \end{cases} \tag{8}$$

with a turnover below $m_0 = 1$ $M_\odot$, and normalized within the mass interval 0.1–100 $M_\odot$ such as $\int m\xi(m)dm = 1$.

In this paper, we assume $\gamma = 2.35$ (a modified Salpeter), but taking $\gamma = 2.2$ ([24]) would not change the final results significantly.

To be consistent with the adopted models of the SFR, we follow [21] and assume a minimal initial mass of 8 $M_\odot$ for NS progenitors, the upper mass being 40 $M_\odot$. It results finally , $\lambda_{\rm NS} = \int_8^{40} \xi(m)dm = 9 \times 10^{-3}$ $M_\odot^{-1}$.

The next step consists to estimate the redshift z_b at which the progenitors have already evolved and the system is now constituted by two neutron stars. This moment fixes also the beginning of the inspiral phase. If τ_b ($\approx 10^8$ yr) is the mean lifetime of the progenitors (average weighted by the IMF in the interval 8–40 $M_\odot$) then

$$z_b = z_f - H_0 \tau_b (1 + z_f) E(z_f). \tag{9}$$

Once the beginning of the inspiral phase is established, the redshift at which the coalescence occurs should now be estimated. The duration of the inspiral depends on the orbital parameters and the neutron star masses. The probability for a given DNS system to coalesce in a timescale τ was initially derived by [25] and confirmed by subsequent simulations [5,26] and is given by

$$P(\tau) = B/\tau. \tag{10}$$

Simulations indicate a minimum coalescence timescale $\tau_0 = 2 \times 10^5$ yr and a considerable number of systems having coalescence timescales higher than the Hubble time. The normalized probability in the range 2×10^5 yr up to 20 Gyr implies $B = 0.087$. Therefore, the redshift z_c at which the coalescence occurs is derived by solving the equation

$$\tau = \tau(z_c, z_b), \tag{11}$$

where

$$\tau(a, b) = \int_a^b \frac{dz}{H_0(1+z)E(z)}. \tag{12}$$

III. THE GRAVITATIONAL WAVE BACKGROUND

Compared with the previous study, slight complications arise when calculating the spectral properties of the signal. In paper II, we were interested in the signal emitted between 10–1500 Hz, which duration in the source frame is short enough, less than 1000 s, to be considered as a burst located at the redshift of coalescence. Now, as we are looking at the inspiral phase in the LISA frequency window (10^{-4}–0.1 Hz), the evolution of the redshift of emission with frequency must be taken into account. For the same reason, the critical redshift at which the population of DNSs constitute a truly continuous background cannot be determined by simply solving the condition $D(z) > 1$, where D is the duty cycle defined as the ratio of the typical duration of a single burst $\bar{\tau}$ to the average time interval

between successive events (see paper II). Instead, we remove the brightest sources, lying in the close Universe, where the distribution of galaxies is expected to be highly anisotropic, in particular, due to the strong concentration of galaxies in the direction of the Virgo cluster and the great attractor (see paper I), and where the density is well below the average value derived from the SFR ([27]). In a second step, we verify that the resulting background is continuous, by using both Jaque Bera and Lilliefors Gaussianity tests with significant level $\alpha = 0.05$ over a set of 100 realizations.

For each realization, the number of simulated DNSs corresponds to the expected number of extragalactic DNSs observed today and is derived as

$$N_p = \int_0^6 N(z)dz. \tag{13}$$

The DNSs present at redshift z were formed at $z_b' \geq z$, with a coalescence time larger than the cosmic time between z_b' and z. Thus,

$$N(z) = \int_z^6 R_{zc}(z')\eta(z')dz', \tag{14}$$

where

$$\eta(z') = \int_{\tau_{\min}}^{\tau_{\max}} P(\tau)d\tau \tag{15}$$

with $\tau_{\max} = 20$ G yr and $\tau_{\min} = \max(2 \times 10^5 \text{ yr}; \tau(z, z_b'))$, which gives $N_p \simeq 1.4 \times 10^6$.

We obtain that after $z_* = 0.005$, corresponding to the distance beyond the Virgo cluster ($\simeq 25$ Mpc), when the relative density fluctuations are <0.5 ([27]), the background is continuous in the range 10^{-4}–0.1 Hz. We consider also a more conservative threshold of $z_* = 0.02$, corresponding to the distance beyond the great attractor ($\simeq$ 100 Mpc), when the relative density fluctuations are <0.05 and when the Universe is expected to become homogeneous ([27,28]).

The gravitational flux in the observer frame produced by a given DNS is

$$f_{\nu_o} = \frac{1}{4\pi d_L^2}\frac{dE_{\rm gw}}{d\nu}(1 + z_e), \tag{16}$$

where z_e is the redshift of emission, $d_L = (1 + z_e)r$ the distance luminosity, r the proper distance, which depends on the adopted cosmology, $dE_{\rm gw}/d\nu$ the gravitational spectral energy and $\nu = (1 + z_e)\nu_o$ the frequency of emission in the source frame.

In the quadripolar approximation and for a binary system with masses m_1 and m_2 in a circular orbit:

$$dE_{\rm gw}/d\nu = K\nu^{-1/3}, \tag{17}$$

where the fact that the gravitational wave frequency is twice the orbital frequency was taken into account. Then

$$K = \frac{(G\pi)^{2/3}}{3}\frac{m_1 m_2}{(m_1 + m_2)^{1/3}}. \tag{18}$$

Taking $m_1 = m_2 = 1.4\ \mathrm{M}_\odot$, one obtains $K = 5.2 \times 10^{50}$ erg Hz$^{-2/3}$.

The redshift of emission is derived by solving the relation [13]:

$$\nu^{-8/3} = \nu_{\rm LSO} + K'(\tau(z_b, z_e)), \tag{19}$$

where

$$K' = \frac{(256\pi^{8/3}G^{5/3})}{5c^5} \tag{20}$$

(or numerically $K' = 67.83$ yr^{-1}), and where the time spent between redshifts z_e and z_b is given by

$$\tau(z_b, z_e) = \tau - \int_{z_c}^{z_e}\frac{dz}{(1 + z)E(z)}. \tag{21}$$

A. Properties of the background

The spectral properties of the stochastic background are characterized by the dimensionless parameter [29]:

$$\Omega_{\rm gw}(\nu_o) = \frac{1}{c^3\rho_c}\nu_o F_{\nu_o}, \tag{22}$$

where ν_o is the wave frequency in the observer frame and ρ_c the critical mass density needed to close the Universe, related to the Hubble parameter H_0 by,

$$\rho_c = \frac{3H_o^2}{8\pi G} \tag{23}$$

F_{ν_o} is the gravitational wave flux at the observer frequency (given here in erg cm^{-2} Hz^{-1} s^{-1}) ν_o, integrated over all sources above the critical redshift z_*, namely

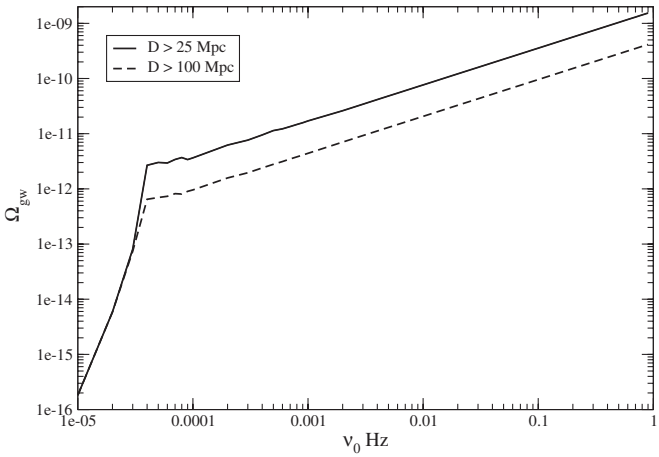

FIG. 1. Spectrum of the expected gravitational energy density parameter $\Omega_{\rm gw}$, corresponding to NS-NS inspirals occurring beyond $d \simeq 25$ Mpc (continuous curve) and $d \simeq 100$ Mpc (dashed curve).

$$F_{\nu_o} = \int_{z_*}^{z_{\max}} f_{\nu_o} dR_c(z). \quad (24)$$

In our simulations, the integrated gravitational flux is calculated by summing individual fluences [Eq. (16)], scaled by the ratio between the total formation rate of progenitors (Eq. (3)) and the number of simulated massive binaries, as

$$F_{\nu_o} = \frac{R_p}{N_p} \sum_{i=1}^{N_p} f^i_{\nu_o}. \quad (25)$$

Figure 1 shows the density parameter $\Omega_{\rm gw}$ as a function of the observed frequency averaged over 10 simulations. The continuous line corresponds to sources located beyond the critical redshift to have a continuous background, $z_* = 0.005$ (or $d \simeq 25$ Mpc), while the dashed line corresponds to the more conservative estimate, with a cutoff at $z_* = 0.02$ (or $d \simeq 100$ Mpc). After a fast increase below $\simeq 5 \times 10^{-5}$ Hz, $\Omega_{\rm gw}$ increases as $\nu_o^{2/3}$ to reach $\Omega_{\rm gw} \simeq 3 \times 10^{-10}$ at 0.1 Hz for $z_* = 0.005$ ($\Omega_{\rm gw} \simeq 10^{-10}$ for $z_* = 0.02$). This is 1 order of magnitude larger than the previous predictions by Schneider *et al.* [13].

B. Consequences for LISA

Astrophysical backgrounds represent a confusion noise for LISA, which spectral density is given by [16]:

$$S_h^{\rm back}(\nu_o) = \frac{3H_0^2}{2\pi^2} \frac{1}{\nu_o^3} \Omega_{\rm gw}(\nu_o). \quad (26)$$

Figure 2 shows $S_h^{\rm back}(\nu_o)$ compared to the LISA sensitivity [30] and to the contribution of unresolved galactic WD-WD [8,30]. The contribution from DNSs may dominate the LISA instrumental noise between $\simeq 3 \times 10^{-4}$–10^{-2} Hz for $z_* = 0.005$ ($\simeq 7 \times 10^{-4}$–6×10^{-3} Hz for $z_* = 0.02$)

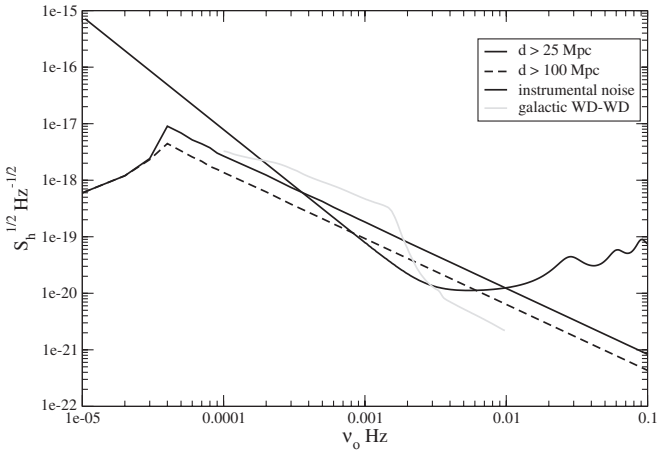

FIG. 2. Gravitational strain in Hz$^{-1/2}$, corresponding to NS-NS inspirals occurring beyond $d \simeq 25$ Mpc (continuous curve) and $d \simeq 100$ Mpc (dashed curve), along with the LISA instrumental noise (black) and the galactic WD-WD foreground (light gray).

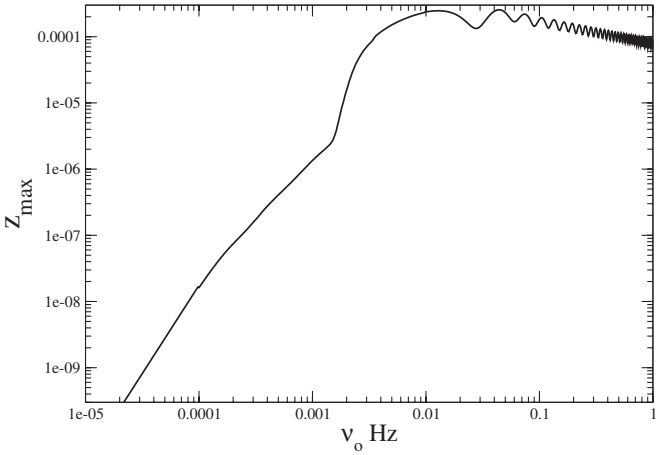

FIG. 3. Maximal redshift as a function of the observed frequency, at which a single DNS can be detected by LISA after 1 yr of integration and with a signal-to-noise ratio $S/R = 5$. The galactic WD-WD foreground is taken into account in the LISA sensitivity.

and the galactic WD-WD confusion noise after $\simeq 2 \times 10^{-3}$. However, the resulting reduction in the sensitivity should be less than a factor 4 and thus should not affect significantly signal detection.

The critical redshift at which a single DNS can be resolved and detected by LISA (Fig. 3) is at least 1 order of magnitude smaller ($z_{\min} \simeq 3 \times 10^{-4}$ at frequencies $\nu_o > 0.01$) than our threshold to have a Gaussian background $z_* = 0.005$ (or $z_* = 0.02$). Sources lying between the two regimes are responsible for a non-Gaussian and nonisotropic cosmic "popcorn" noise (see [31] for a recent review) that will be investigated in a further work. This contribution, which statistical properties differ from those of both the instrumental noise and the cosmological background, could be detected and removed by new data analysis techniques currently under investigation, such as the search for anisotropies [32] that can be used to create a map of the GW background [33,34], the maximum likelihood statistic [35], or methods based on the probability event horizon concept [36], which describes the evolution, as a function of the observation time, of the cumulated signal throughout the Universe.

IV. CONCLUSIONS

In this paper, we have modeled the contribution of extra galactic inspiralling double neutron stars, to the to the astrophysical gravitational wave foreground, in the range of sensitivity of the space detector LISA.

Using a recent fit of the star formation rate [21], optimized for a top heavy A modified Salpeter IMF, we show that sources beyond $z_* = 0.005$ (or $z_* = 0.02$ for a more conservative estimate) constitute a truly continuous background. We find that the density parameter $\Omega_{\rm gw}$, after a fast increase below $\simeq 5 \times 10^{-5}$ Hz, increases as $\nu_o^{2/3}$ to reach

$\Omega_{gw} \simeq 3 \times 10^{-9}$ ($\Omega_{gw} \simeq 10^{-10}$) at 0.1 Hz, which is 1 order of magnitude above the previous estimate of [13]. As a result, the signal may dominate the LISA instrumental noise in the range $\simeq 3 \times 10^{-4}$–10^{-2} Hz ($\simeq 7 \times 10^{-4}$–6×10^{-3}) and overwhelm the galactic WD-WD confusion noise at frequencies larger than $\nu_o \simeq 2 \times 10^{-3}$. Sources located closer than z_*, but still too far to be detected by LISA, constitute a non-Gaussian and nonisotropic cosmic popcorn noise, which will be investigated in a further work.

ACKNOWLEDGMENTS

The author thanks J. A. de Freitas Pacheco and A. Spallicci for useful discussions, which have improved the first versions of the paper.

[1] C. Bradaschia *et al.*, Nucl. Instrum. Methods Phys. Res., Sect. A **289**, 518 (1990).
[2] A. Abramovici *et al.*, Science **256**, 325 (1992).
[3] J. Hough, in *Proceedings of the Sixth Marcel Grossmann Meeting*, edited by H. Sato and T. Nakamura (World Scientific, Singapore, 1992), p. 192.
[4] K. Kuroda *et al.*, in *Proceedings of the International Conference on Gravitational Waves: Sources and Detectors, 1997*, edited by I. Ciufolini and F. Fidecaro (World Scientific, Singapore, 1997), p. 1007.
[5] J. A. de Freitas Pacheco, T. Regimbau, A. Spallicci, and S. Vincent, Int. J. Mod. Phys. D **15**, 235 (2006).
[6] T. Regimbau and J. A. de Freitas Pacheco, Astrophys. J. **642**, 455 (2006).
[7] C. R. Evans, I. Iben, and L. Smarr, Astrophys. J. **323**, 129 (1987).
[8] D. Hils, P. L. Bender, and R. F. Webbink, Astrophys. J. **360**, 75 (1990).
[9] P. L. Bender and D. Hils, Classical Quantum Gravity **14**, 1439 (1997).
[10] K. A. Postnov and M. E. Prokhorov, Astrophys. J. **494**, 674 (1998).
[11] G. Neleman, L. Yungelson, and S. F. Potergies Zwart, Astron. Astrophys. **375**, 890 (2001).
[12] S. E. Timpano, L. J. Rubbo, and N. J. Cornish, Phys. Rev. D **73**, 122001 (2006).
[13] R. Schneider, V. Ferrari, S. Matarrese, and S. F. Potergies Zwart, Mon. Not. R. Astron. Soc. **324**, 797 (2001).
[14] A. J. Farmer and E. S. Phinney, Mon. Not. R. Astron. Soc. **386**, 1197 (2003).
[15] A. Cooray, Mon. Not. R. Astron. Soc. **354**, 25 (2004).
[16] L. Barack and C. Cutler, Phys. Rev. D **70**, 122002 (2004).
[17] D. Coward, R. R. Burman, and D. Blair, Mon. Not. R. Astron. Soc. **329**, 411 (2002).
[18] S. M. Rao, D. A. Turnshek, and D. B. Nestor, Astrophys. J. **636**, 610 (2006).
[19] Spergel *et al.*, Astrophys. J. Suppl. Ser. **148**, 175 (2003).
[20] S. Cole *et al.*, Mon. Not. R. Astron. Soc. **326**, 255 (2001).
[21] A. M. Hopkins, J. Beacom, astro-ph/0601463.
[22] C. Porciani and P. Madau, Astrophys. J. **548**, 522 (2001).
[23] E. E. Salpeter, Astrophys. J. **121**, 161 (1955).
[24] I. Baldry and K. Glazebrook, Astrophys. J. **593**, 258 (2003).
[25] J. A. de Freitas Pacheco, Astropart. Phys. **8**, 21 (1997).
[26] S. Vincent, DEA Dissertation, University of Nice-Sophia Antipolis, France, 2002.
[27] J. A. de Freitas Pacheco, "*Lectures on Physical Cosmology*," University of Nice-Sophia Antipolis, France 2006 (unpublished).
[28] X. P. Wu, B. Qin, and L. Z. Fang, Astrophys. J. **469**, 48 (1996).
[29] V. Ferrari, S. Matarrese, and R. Schneider, Mon. Not. R. Astron. Soc. **303**, 258 (1999).
[30] S. L. Larson, Online Sensitivity Curve Generator, located at http://www.srl.caltech.edu/ shane/sensitivity/; S. L. Larson, W. A. Hiscock, and R. W. Hellings, Phys. Rev. D **62**, 062001 (2000).
[31] D. Coward and T. Regimbau, New Astron. Rev. **50**, 461 (2006).
[32] B. Allen and A. C. Ottewill, Phys. Rev. D **56**, 545 (1997).
[33] N. J. Cornish, Classical Quantum Gravity **18**, 4277 (2001).
[34] S. Ballmer, Classical Quantum Gravity **23**, S179 (2006).
[35] S. Drasco and E. E. Flanagan, Phys. Rev. D **67**, 082003 (2003).
[36] D. Coward and R. R. Burman, Mon. Not. R. Astron. Soc. **361**, 362 (2005).